




Cite this: *Soft Matter*, 2024, 20, 5237

Received 22nd March 2024,
Accepted 4th June 2024

DOI: 10.1039/d4sm00338a

rsc.li/soft-matter-journal

Extremely persistent dense active fluids

Grzegorz Szamel* and Elijah Flenner 

We study the dynamics of dense three-dimensional systems of active particles for large persistence times τ_p at constant average self-propulsion force f . These systems are fluid counterparts of previously investigated extremely persistent systems, which in the large persistence time limit relax only on the time scale of τ_p . We find that many dynamic properties of the systems we study, such as the mean-squared velocity, the self-intermediate scattering function, and the shear-stress correlation function, become τ_p -independent in the large persistence time limit. In addition, the large τ_p limits of many dynamic properties, such as the mean-square velocity and the relaxation times of the scattering function, and the shear-stress correlation function, depend on f as power laws with non-trivial exponents. We conjecture that these systems constitute a new class of extremely persistent active systems.

1 Introduction

Self-propelled or active particles, which use energy from their environment to perform persistent motion, behave in surprising and interesting ways.^{1–3} Recently, novel intermittent dynamics was identified in extremely persistent dense homogeneous two-dimensional systems.^{4–7} These systems were shown to relax on the time-scale of the persistence time τ_p by going through sequences of mechanical equilibria in which self-propulsion forces balance interparticle forces. In contrast, at low and moderate densities and long persistence times active matter undergo motility-induced phase separation (MIPS), and separate into regions with dramatically different densities.

Here we examine the fluid counterparts of systems considered in ref. 4–7; extremely persistent homogeneous three-dimensional active fluids in which the interparticle interactions never manage to balance the self-propulsion forces, which influence particles' motion in a nontrivial way. Although our fluid systems are less dense than those considered in ref. 4–7, they are dense enough such that we do not observe MIPS.

The parameter space of active systems is much larger than that of passive ones. At a minimum, one has to specify the average strength of active forces and their persistence time in addition to the set of parameters characterizing the corresponding passive system. If one considers athermal active systems, this results in a three-dimensional control parameter space. Thus, when comparing results of diverse studies, one needs to specify the path in the parameter space that one is following.

Early studies of dense homogeneous active systems focused on the glassy dynamics and the active glass transition.^{8–17} Many

of these studies considered a limited range of persistence times and often examined the behavior at constant active temperature T_a that characterizes the long-time motion of an isolated active particle. For many models of self-propulsion, with increasing τ_p at constant T_a , the strength of active forces decreases and dense active systems typically become glassy, see Fig. 2(c) of ref. 6 for a recent example. Thus, to investigate the effects of extremely persistent active forces it is common to fix the force strength while increasing the persistence time.^{4,5,7}

Recently, it has been shown that interesting behavior emerges for large persistence times in dense active particle systems.^{4–7,18} First, it was found that some extremely persistent dense active systems relax only on the time scale of τ_p .^{4–7} In these systems, the mean squared displacement (MSD) and the two-point overlap function exhibit well-defined large τ_p limits when plotted *versus* time rescaled by the persistence time.⁵ Distributions of velocity components were found to exhibit fat exponential tails.⁶ An intermediate-time plateau in the MSD was absent. Instead, a region of super-diffusive MSD scaling with time as t^β with $\beta \approx 1.6$ for times less than τ_p was identified.⁶

Second, a recent study of two-dimensional active systems that remain fluid in the large persistence time limit showed that mesoscale advective flows, forming streams and vortices, emerge for large persistence times.¹⁸ These flow patterns resemble turbulent flows, and thus this phenomenon was identified as a type of “active turbulence”.

Here we study dense homogeneous three-dimensional active systems that do not undergo dynamic arrest in the large persistence time limit. In contrast to findings of ref. 4–7, for large persistence times τ_p many dynamic properties of our systems become τ_p -independent and their relaxation functions exhibit well-defined limits when plotted *versus* time not scaled by the persistence time. Also, the large persistence time limits

Department of Chemistry, Colorado State University, Fort Collins, CO, USA.
E-mail: grzegorz.szamel@colostate.edu



of many properties depend on the strength of active forces f as power laws. We emphasize that both the active systems studied in ref. 4–7 and the fluid-like active systems studied here exhibit universal behavior, but on very different time scales.

It could be surmised that, in the infinite τ_p limit, our systems lie in the un-jammed phase of the active yielding phase diagram studied (in two dimensions) by Liao and Xu.¹⁹ However, these authors studied systems of particles interacting *via* a harmonic repulsion, in which interparticle forces are bounded, and thus strong enough self-propulsion forces are always able to induce motion. In contrast, in our systems interparticle forces are un-bounded, and thus their jamming phase diagram may be different from that obtained by Liao and Xu.

2 Simulations

We study a three-dimensional 50:50 binary mixture of spherically symmetric active particles interacting *via* the Weeks–Chandler–Andersen²⁰ potential,

$$V_{\alpha\beta} = 4\epsilon \left[\left(\frac{\sigma_{\alpha\beta}}{r} \right)^{12} - \left(\frac{\sigma_{\alpha\beta}}{r} \right)^6 \right] \quad (1)$$

for $r < \zeta_{\alpha\beta} = 2^{1/6}\sigma_{\alpha\beta}$ and 0 otherwise. Here, α, β denote the particles species A or B and ϵ is the unit of energy. The distance unit is set by $\sigma_{BB} = 1.0$, $\sigma_{AA} = 1.4$, and $\sigma_{AB} = 1.2$. We study the number density $N/V = 0.451$, which corresponds to the volume fraction $\phi = \pi N[\zeta_{AA}^3 + \zeta_{BB}^3]/(12V) = 0.625$.

We use the athermal active Ornstein–Uhlenbeck particle model without thermal noise.^{21–23} The equation of motion for the position \mathbf{r}_n of particle n is

$$\zeta_0 \dot{\mathbf{r}}_n = \mathbf{F}_n + \mathbf{f}_n, \quad (2)$$

where $\mathbf{F}_n = -\sum_{m \neq n} \nabla_n V(r_{nm})$ and \mathbf{f}_n is the active force. $\zeta_0 = 1$ is the friction coefficient of an isolated particle and $\zeta_0 \sigma_{BB}^2/\epsilon$ sets the unit of time.

In turn, the self-propulsion forces evolve according to the Ornstein–Uhlenbeck process. The equation of motion for the self-propulsion force acting on particle n reads

$$\tau_p \dot{\mathbf{f}}_n = -\mathbf{f}_n + \zeta_n, \quad (3)$$

where τ_p is the persistence time of the self-propulsion and ζ_n is a Gaussian white noise with zero mean and variance $\langle \zeta_n(t) \zeta_m(t') \rangle_{\text{noise}} = 2\zeta_0 T_a \mathbf{I} \delta_{nm} \delta(t - t')$, where $\langle \dots \rangle_{\text{noise}}$ denotes averaging over the noise distribution, T_a is a single particle effective temperature, \mathbf{I} is the unit tensor and we set the Boltzmann constant $k_B = 1$. The root-mean square strength of active forces is $f = \sqrt{3T_a/\tau_p}$. The time step for the simulations ranged from 0.01 to 0.0001 with a smaller time step needed for larger f and longer τ_p . We simulated at least $10\tau_p$ for each of 4 production runs, which required up to 10^9 time steps.

To check for finite size effects we studied systems of 1k, 8k, and 64k particles at large persistence times. We did not find any system size dependence of the system's dynamics or properties. The results shown in this work are for 1K particles unless otherwise noted in the figure caption.

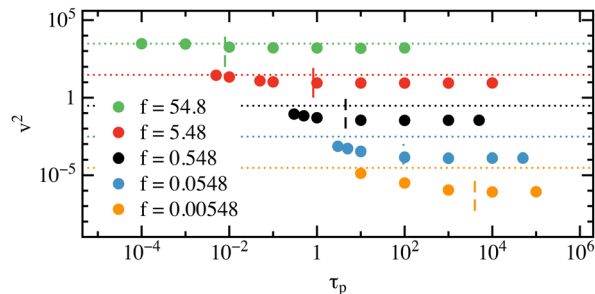


Fig. 1 The persistence time dependence of the mean squared velocity $v^2 = \langle \dot{\mathbf{r}}^2 \rangle$ for fixed active force strength f . The velocity decreases and then saturates. The vertical dashed lines indicate approximate τ_p at which the saturation occurs. The dotted lines are the free particle value of $v^2 = f^2$ for each corresponding color.

3 Single-particle dynamics

We start by examining the persistence time dependence of the mean square velocity, $v^2 \equiv N^{-1} \langle \sum_n \dot{\mathbf{r}}_n^2 \rangle = N^{-1} \langle \sum_n \mathbf{F}_n^2 + \sum_n 2\mathbf{F}_n \cdot \mathbf{f}_n \rangle + f^2$, which is shown in Fig. 1. With increasing persistence time v^2 decreases and then saturates. For the range of f that we studied, the cancellation of the interparticle and active forces is never complete and the system does not become arrested on the time scale of the persistence time.^{5,7}

Next, we examine the persistence time dependence of the MSD

$$\langle \delta r^2(t) \rangle = N^{-1} \left\langle \sum_n [\mathbf{r}_n(t) - \mathbf{r}_n(0)]^2 \right\rangle, \quad (4)$$

shown in Fig. 2. At short times the motion is ballistic and it is determined by v^2 , $\langle \delta r^2(t) \rangle \approx v^2 t^2$.¹¹ For large persistence times the short-time dynamics become τ_p -independent, which confirms saturation of v^2 . For small τ_p and fixed f we observe a well developed intermediate time plateau crossing over to diffusive behavior at long times. This behavior, characteristic of a system close to dynamic arrest, can be understood by noticing that the state point $f = 5.48$, $\tau_p = 0.001$ is the same as the state point $T_{\text{eff}} = 0.01$, $\tau_p = 0.001$ of

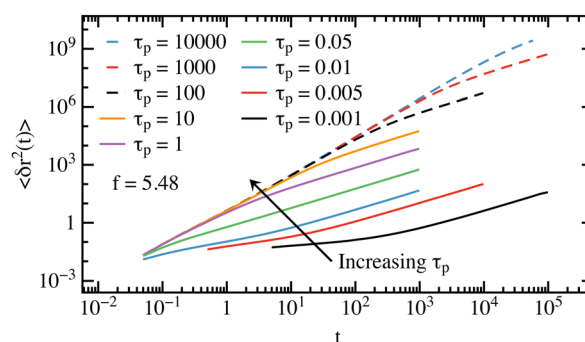


Fig. 2 The mean squared displacement (MSD) $\langle \delta r^2(t) \rangle$ for $f = 5.48$ and several τ_p . For shorter τ_p MSDs display a glassy plateau followed by diffusive motion. With increasing τ_p an extended superdiffusive region appears that is analyzed in Fig. 4(a).



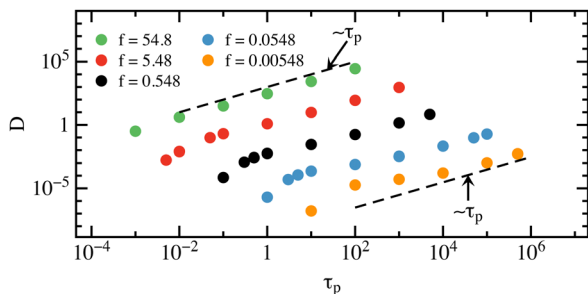


Fig. 3 The long time diffusion coefficient D for fixed active force strength f as a function of persistence time. D grows with increasing τ_p and is proportional to τ_p in the large τ_p limit.

ref. 17. Fig. 2(c) and 3 of the latter paper show that this state point is on the fluid side of the glass phase diagram, very close to the dynamic arrest line. With increasing τ_p the intermediate time plateau characteristic of glassy dynamics disappears and the system becomes more fluid like. Similar fluidization with increasing τ_p and fixed f was observed in two-dimensional systems by Paoluzzi *et al.*²⁴

At long times, the MSD exhibits diffusive behavior. The self-diffusion coefficient, $D = \lim_{t \rightarrow \infty} \langle \delta r^2(t) \rangle / (6t)$, is shown in Fig. 3. For a given f it monotonically increases with increasing τ_p . At large τ_p we find that $D \sim \tau_p$, indicated by the dashed lines.

We find a surprising time-dependence of the MSD between the initial ballistic and the long-time diffusive regimes. In Fig. 4(a) we show the MSD divided by $v^2 t^2$ to show this time-dependence more clearly. The MSD exhibits a superdiffusive behavior that does not follow a single power law. Instead, a second, intermediate time ballistic regime appears, with velocity v_1 . In the $\tau_p \rightarrow \infty$ limit the system stays in the second ballistic regime.

The time-dependence of the MSD shown in Fig. 4(a) is reflected in the time-dependence of the velocity auto-correlation

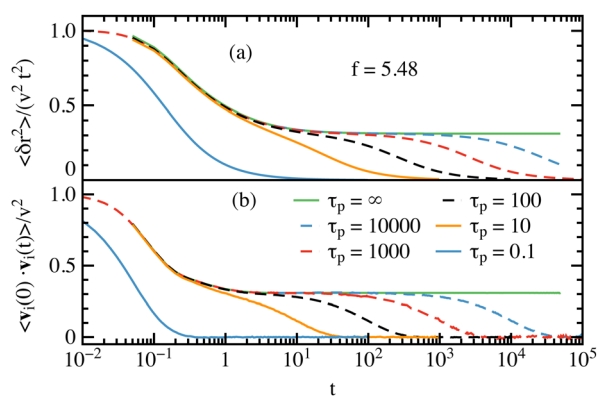


Fig. 4 (a) The mean squared displacement divided by $v^2 t^2$ for $f = 5.48$. For large τ_p , at short times the motion is ballistic (not shown), and then there is a super-diffusive regime. For very large τ_p the super-diffusive motion speeds up and the resulting behavior is approximately ballistic. For $t > \tau_p$ long-time diffusive motion is observed. In the $\tau_p \rightarrow \infty$ limit the system stays in the second ballistic regime, with velocity v_1 . (b) The velocity autocorrelation function. For very large τ_p an intermediate time plateau is observed. The level of the plateau is the same in both panels.

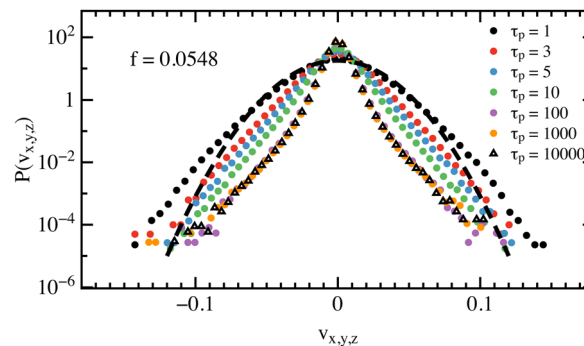


Fig. 5 The distribution of velocities for $f = 0.0548$ for a range of persistence times. The distributions are non-Gaussian; the tails become more prominent with increasing τ_p until the persistence time at which v^2 saturates and then the distributions overlap. The dashed line represents a Maxwell distribution.

function, $VACF(t) = N^{-1} \sum_n \langle \dot{\mathbf{r}}_n(t) \cdot \dot{\mathbf{r}}_n(0) \rangle$, shown in Fig. 4(b). We observe a two-step decay, which becomes increasingly more pronounced with increasing τ_p . This agrees with the observation in ref. 18, except that, since we keep strength of active forces f constant, we find the plateau level to be τ_p independent. We note that the plateau levels are the same in both panels of Fig. 4. The plateau level decreases with increasing self-propulsion force f .

Results shown in Fig. 4 suggest that, in the large τ_p limit, the diffusion can be thought of as a random walk consisting of steps of length $v_1 \tau_p$ taken every τ_p . This reasoning rationalizes the observed scaling $D \sim \tau_p$. We note that while the physical picture of a random walk of steps of length $v_1 \tau_p$ taken every τ_p is identical to the behavior expected at low densities, our systems exhibit highly non-trivial dependence of v_1 on the average self-propulsion force f , which we will discuss at the end of this section. This dependence suggests that the observed effective behavior is strongly influenced by interparticle interactions.

In Fig. 5 we show velocity distributions. As found by Keta *et al.*,⁶ the distributions are strongly non-Gaussian. Their broad tails become more prominent with increasing τ_p and then saturate.

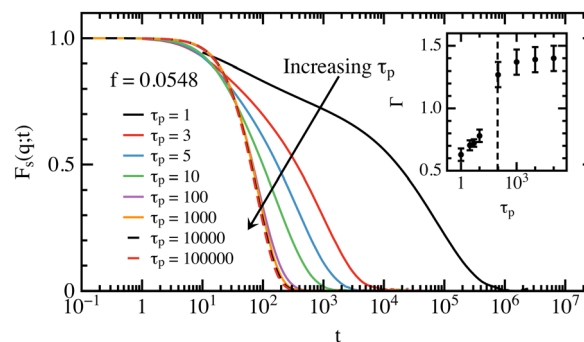


Fig. 6 The self-intermediate scattering function $F_s(k; t)$ for $f = 0.0548$ and a range of persistence times. The relaxation time decreases with increasing persistence time until around $\tau_p(f)$ where $F_s(k; t)$ becomes independent of persistence time. The inset shows the τ_p dependence of parameter Γ of fit to $F_s(k; t) = a e^{-(t/\tau_s)^\Gamma}$.



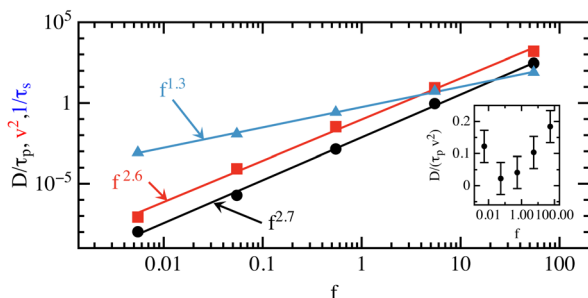


Fig. 7 The large τ_p limit of v^2 , D/τ_p and $1/\tau_s$ as a function of the self-propulsion strength f . The lines are power law fits where the exponent for v^2 , D/τ_p and $1/\tau_s$ are 2.6 ± 0.1 , 2.7 ± 0.1 and 1.3 ± 0.1 , respectively. The inset shows $D/(\tau_p v^2)$ versus f , which varies between 0.02 to 0.2 over the range of f examined, with error bars of about 0.05.

The evolution of the MSD with the persistence time is reflected in the τ_p dependence of the self-intermediate scattering function

$$F_s(k; t) = \frac{1}{N} \left\langle \sum_n e^{ik \cdot (\mathbf{r}_n(t) - \mathbf{r}_n(0))} \right\rangle. \quad (5)$$

We chose $k = 5.3$, which is approximately equal the first peak of the total static structure factor. In Fig. 6 we show $F_s(k; t)$ for $f = 0.0548$. With increasing τ_p the intermediate time glassy plateau disappears and the decay changes from stretched exponential, to exponential, then to compressed exponential. Shown in the inset to Fig. 6 is the parameter Γ obtained from fits to $F_s(k; t) = ae^{-(t/\tau_s)^\Gamma}$ where we restrict $a \leq 1$. Γ increases with increasing τ_p and reaches a plateau above $\tau_p \approx 94$.

We find that the large persistence time limits of several properties discussed above depend on the strength of the active forces as power laws. In Fig. 7 we show the large τ_p limits of v^2 (squares), D/τ_p (circles) and τ_s (triangles). We find that the former two quantities follow a power law with f with statistically the same exponent, 2.6 ± 0.1 for v^2 and 2.5 ± 0.1 for D/τ_p . We note that v^2 is bound from above by f^2 , which corresponds to the limit in which interactions become irrelevant compared to active forces. Thus, we do not expect the power law for v^2 to extend up to arbitrary large f . The power law of the relaxation time, $\tau_s \sim f^{-1.3}$ can be related to

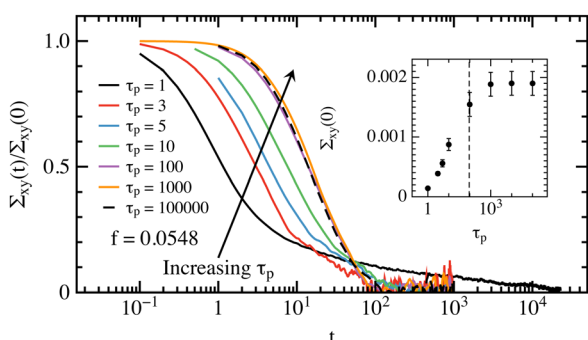


Fig. 8 Normalized shear-stress correlation function for $f = 0.0548$ and a range of persistence times. The shear stress relaxation time initially increases with τ_p , and then saturates. Additionally, $\Sigma_{xy}(0)$ grows with τ_p and then it becomes approximately constant (inset).

that of v^2 ; in the large τ_p limit F_s decays on the time scale on which a particle moves over its diameter, which scales as v .

We also analyzed the dependence of v_1 on the strength of the active forces. To this end, we extracted v_1^2 for each f by finding the plateau in $\langle \delta r^2(t) \rangle / t^2$ for large τ_p . We find that v_1^2 grows with f as a power law with an exponent of 2.5 ± 0.2 , which is statistically the same as the exponent for v^2 .

We emphasize that, although in the large τ_p limit the motion of individual particles is close to ballistic, it is still influenced by the interparticle interactions in a highly non-trivial way. If there were no interparticle interactions, scaling exponents discussed above would have values 2 and -1 .

4 Collective dynamics

The quantities discussed in Section 3 describe the single particle motion in our many-particle systems. To examine collective properties we investigated the persistence time dependence of the stress fluctuations and the rheological response. First, we examined the shear-stress correlation function $\Sigma_{\alpha\beta}(t) = V^{-1} \langle \sigma_{\alpha\beta}(t) \sigma_{\alpha\beta}(0) \rangle$, where

$$\sigma_{\alpha\beta}(t) = -\frac{1}{2} \sum_n \sum_{m \neq n} \frac{r_{nm}^\alpha r_{nm}^\beta}{r_{nm}} \frac{dV(r_{nm})}{dr_{nm}}, \quad (6)$$

and r_{nm}^α is the α component of the distance vector between particle n and particle m .

In Fig. 8 we report the normalized shear stress correlation function, $\Sigma_{xy}(t)/\Sigma_{xy}(0)$, for $f = 0.0548$ and a large range of τ_p . For small τ_p there is a rapid decay to an emerging plateau followed by a slow decay to zero. With increasing persistence time, the decay of $\Sigma_{xy}(t)$ becomes less stretched; it is exponential for a long enough τ_p . In the inset we show the dependence of the initial value, $\Sigma_{xy}(0)$, on τ_p . We see that the initial value first grows with τ_p and then plateaus.

To probe the rheological response of our active systems we simulated shear flow by adding to the equations of motion (2) a bulk non-conservative force $\mathbf{F}_n^i = \xi_0^i \gamma_n \mathbf{e}_x$ with Lees-Edwards boundary conditions.²⁵ In Fig. 9 we show the average shear stress, $\langle \sigma_{xy} \rangle / \dot{\gamma}$, for $f = 0.548$ and a large range of τ_p . In Fig. 10 we show the τ_p dependence of the zero-shear-rate viscosity

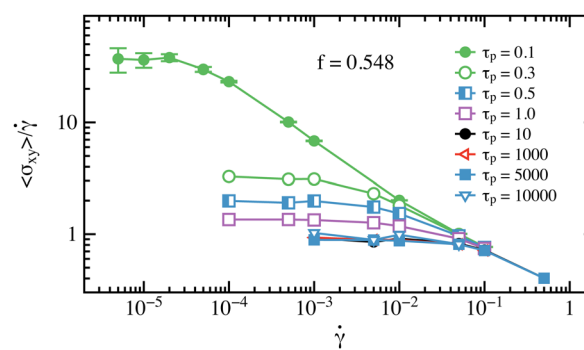


Fig. 9 Average shear stress $\langle \sigma_{xy} \rangle$ divided by the shear rate $\dot{\gamma}$ at constant $f = 0.548$ for a range of persistence times. The zero-shear-rate viscosity η can be obtained from the small shear rate plateau.



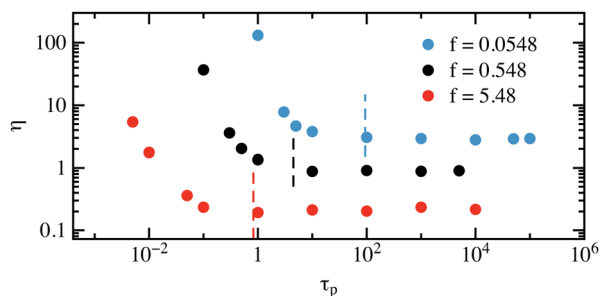


Fig. 10 The viscosity η at fixed average active forces strength versus τ_p . The viscosity initially decreases with increasing τ_p and then becomes constant. The vertical dashed lines indicate approximate τ_p at which the saturation occurs.

obtained from the small $\dot{\gamma}$ plateaus of $\langle \sigma_{xy} \rangle / \dot{\gamma}$. We find that η initially decreases and reaches a τ_p -independent plateau.

We find that large τ_p limits of collective properties also scale with f as power laws. In Fig. 11 we show the dependence of the large τ_p limits of the relaxation time of the normalized stress tensor autocorrelation function and of the viscosity on the strength of the self-propulsion.

5 Static structure

When analyzing the dynamics in passive systems, one usually tries to make connections between the average distribution of the particles and their dynamics. To check how the average arrangement of the particles in our active systems changes with increasing τ_p we evaluated the total steady-state structure factor

$$S(k) = \frac{1}{N} \left\langle \sum_{n,m} e^{i\mathbf{k} \cdot (\mathbf{r}_n - \mathbf{r}_m)} \right\rangle, \quad (7)$$

with summation over all particles in the system, and the pair correlation function between the large particles,

$$g(r) = \frac{V}{(N/2)^2} \left\langle \sum_n \sum_{m \neq n} \delta(\mathbf{r} - (\mathbf{r}_n - \mathbf{r}_m)) \right\rangle, \quad (8)$$

where the summation extends over the large particles only.

In Fig. 12 we show that the peak height of $S(k)$ initially decreases with increasing τ_p , which nicely correlates with

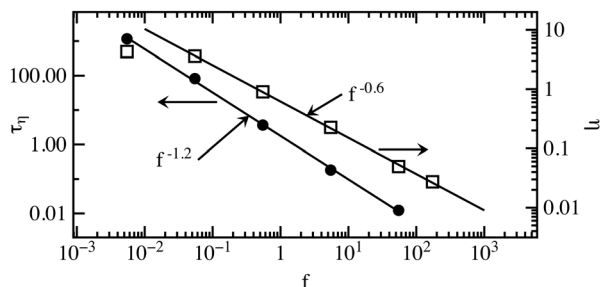


Fig. 11 The large τ_p limit of the relaxation time of $\Sigma_{xy}(t)/\Sigma_{xy}(0)$ (defined as when this function equals e^{-1}) and of viscosity η as a function of the self-propulsion strength f . The lines are power law fits where the exponents for τ_r and η are -1.2 ± 0.1 and -0.60 ± 0.1 , respectively.

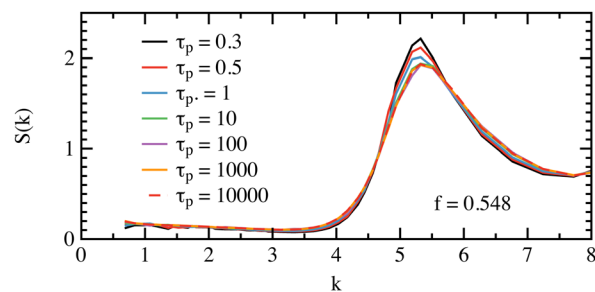


Fig. 12 The persistence time dependence of the steady-state structure factor $S(k)$ for $f = 0.548$. The peak height decreases with increasing persistence time and then saturates at a large persistence time.

relaxation getting faster and viscosity decreasing. The peak height then saturates at a large persistence time. The large τ_p limit of the structure factors still looks liquid-like, and thus it does not signal the interesting dynamics we uncovered. To describe the dynamics of extremely persistent dense active fluids one cannot rely upon static structure factors only.

We note that the absence of any small wavevector peak implies that our systems are homogeneous. We confirmed this observation by evaluating local density histograms at several simulated state points. Incidentally, the homogeneity allows us to rationalize the absence of shear thickening that was observed

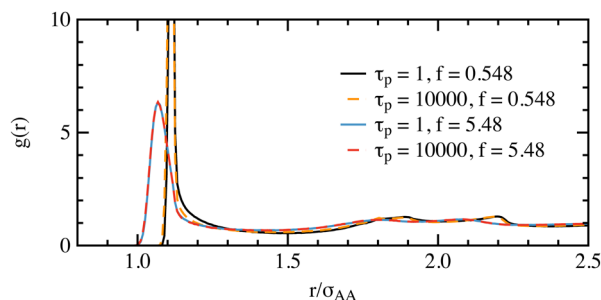


Fig. 13 The pair correlation function between the large particles for $f = 0.548$ and $f = 5.48$ and two representative persistence times $\tau_p = 1$ and $\tau_p = 10000$. For small f the first peak in $g(r)$ is sharply peaked; it is shown in Fig. 14. There is little dependence of $g(r)$ on the persistence time.

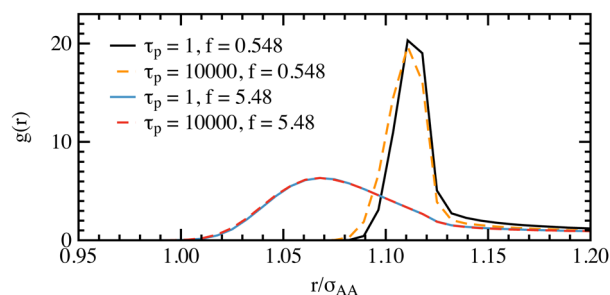


Fig. 14 The first peak of the pair correlation function between the large particles for $f = 0.548$ and $f = 5.48$ and two representative persistence times $\tau_p = 1$ and $\tau_p = 10000$. The peak height decreases and the peak width increases with increasing f . There is little dependence of the first peak of $g(r)$ on the persistence time.



at large self-propulsions in ref. 26, which was attributed to clustering and was dubbed motility-induced shear thickening.

In Fig. 13 and 14 we show the pair correlation function between the large particles. In contrast to the behavior exhibited by the structure factor, $g(r)$ is not very sensitive to the changes in the persistence time. However, the height of the first peak of $g(r)$ decreases rapidly with increasing self-propulsion force f while the position of the first peak shifts to the smaller r , suggesting that the system becomes effectively less crowded with increasing f . This rationalizes decreasing large persistence time limits of the relaxation times and of the viscosity and increasing large persistence time limit of the diffusion coefficient.

6 Conclusions

We conjecture that the systems we presented here form a new class of extremely persistent active matter systems. Earlier investigations^{5,7} revealed systems that relax on the time scale of the self-propulsion and exhibit intermittent dynamics. The systems with intermittent dynamics slow down with increasing τ_p at fixed f , but they exhibit universal dynamics when investigated as a function of time rescaled by τ_p . In contrast, the systems we presented exhibit universal dynamics for large τ_p but as a function of un-scaled time. We expect that for higher volume fractions there is a transition between the regime in which the relaxation becomes independent of the persistence time of the self-propulsion, which is the regime we analyzed, and the regime in which the system flows only on the time scale of the self-propulsion, which is the regime investigated earlier.^{5,7} At a fixed strength of the active forces the transition is driven by the density. Since interparticle interactions in our systems are not bounded, it is not obvious whether, at constant density, the transition can be induced by changing the force strength, like in two-dimensional systems with harmonic interactions, which were investigated by Liao and Xu.¹⁹

For the systems studied here, the single-particle motion exhibits two ballistic regions separated by a superdiffusive regime. Classic signatures of two-step relaxation seen in glassy systems are absent both in the MSD and $F_s(k;t)$. Therefore, our systems are not close to a glass transition. Many properties that quantify the large persistence time limit of the relaxation depend on the strength of the active forces as a power law.

In contrast to Keta *et al.*,¹⁸ we did not observe essential features of “active turbulence”. In particular, mean-squared displacement difference of initially close by particles monitored by Keta *et al.* was only slightly smaller than the MSD. This may not be surprising since our systems have somewhat lower density and larger active forces.

Finally, we note that approximate theories developed to describe the relaxation in active fluids^{27–32} we tested against computer simulations for rather limited range of self-propulsion force f and persistence time τ_p . The discovery of a new paradigm of extremely persistent active fluids with non-trivial power laws calls for additional theoretical work. The single-particle motion in the systems that we investigated can

perhaps be described as a persistent random walk with renormalized density and self-propulsion-dependent velocity. However, it is unlikely that such a simple picture could also account for the collective dynamic properties.

Data availability

Data for this article is available on Dryad at <https://doi.org/10.5061/dryad.xsj3tx9q4>.

Conflicts of interest

There are no conflicts to declare.

Appendices

Motility induced phase separation (MIPS) is often reported and extensively studied in active systems. In two-dimensional systems it has been shown that MIPS will occur with increasing τ_p and fixed f over a range of densities.²⁴ We note that, in three-dimensional systems states with MPIS, coexistence is metastable with respect to active crystallization in a large region of the parameter space.³³ Here we claim that our system is not undergoing MIPS at any of the state points studied.

To determine if the system undergoes MIPS one can examine structural signatures and density distributions. One structural signature is an upturn of the structure factor $S(k)$ at small wavevectors k . However, an upturn can occur if there are large density fluctuations but no MIPS. The density distribution is another method to examine MIPS, where two peaks indicate that the system has separated into high density and low density regions. We use these two methods.

To calculate the density distribution we divide the system into boxes of length $\ell = 2.6082$ and determine the density inside each box. For each configuration used in the calculation we determine the density distribution of the small boxes and then

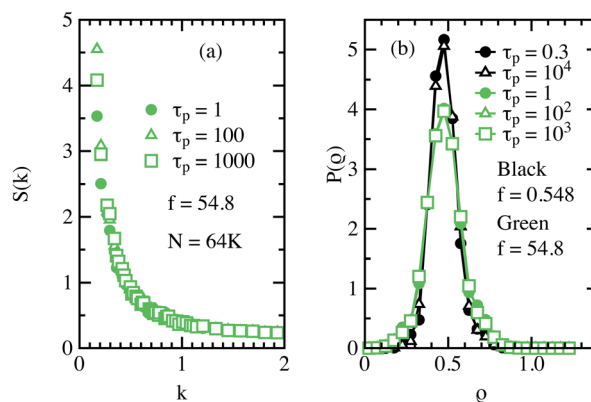


Fig. 15 (a) The structure factor $S(k)$ for $f = 54.8$ for our 64k system. There is a distinct upturn at small wavevectors which is not seen for our other f . (b) The density distribution for the same f , N , and τ_p as shown in (a), and for two state points for which structure factors were shown in Fig. 12. We do not observe the two peak structure expected for systems undergoing motility induced phase separation.



average these distributions. To examine smaller wavevectors and to get a more accurate density distribution we present results for our 64k systems.

As shown in Fig. 12 we don't see any evidence of an upturn in the low wavevector values of $S(k)$ for $f = 0.548$. The only f we do observe an upturn at small wavevectors is $f = 54.8$, Fig. 15(a). We note that the small k upturn does not increase with increasing τ_p , and thus we don't expect any changes with increasing τ_p . The density distribution for these state points do not show a two peak structure and remains statistically unchanged when increasing τ_p , Fig. 15(b). We conclude that there are large density fluctuations, but the system is not yet undergoing MIPS. For larger f we expect that this system will exhibit MIPS.

Acknowledgements

We thank L. Berthier and P. Sollich for discussions and comments on the manuscript. Part of this work was done when GS was on sabbatical at Georg-August Universität Göttingen. He thanks his colleagues there for their hospitality. We gratefully acknowledge the support of NSF Grant No. CHE 2154241.

Notes and references

- M. C. Marchetti, J. F. Joanny, S. Ramaswamy, T. B. Liverpool, J. Prost, M. Rao and R. Aditi Simha, "Hydrodynamics of soft active matter", *Rev. Mod. Phys.*, 2013, **85**, 1143–1189.
- J. Elgeti, R. G. Winkler and G. Gompper, "Physics of microswimmers-single particle motion and collective behavior: a review", *Rep. Prog. Phys.*, 2015, **78**, 056601.
- C. Bechinger, R. Di Leonardo, H. Löwen, C. Reichhardt, G. Volpe and G. Volpe, "Active particles in complex and crowded environments", *Rev. Mod. Phys.*, 2016, **88**, 045006.
- R. Mandal, P. J. Bhuyan, P. Chaudhuri, C. Dasgupta and M. Rao, "Extreme active matter at high densities", *Nat. Commun.*, 2020, **11**, 2581.
- R. Mandal and P. Sollich, "How to study a persistent active glassy system", *J. Phys.: Condens. Matter*, 2021, **33**, 184001.
- Y.-E. Keta, R. L. Jack and L. Berthier, "Disordered Collective Motion in Dense Assemblies of Persistent Particles", *Phys. Rev. Lett.*, 2022, **129**, 048002.
- Y.-E. Keta, R. Mandal, P. Sollich, R. L. Jack and L. Berthier, "Intermittent relaxation and avalanches in extremely persistent active matter", *Soft Matter*, 2023, **19**, 3871–3883.
- L. Berthier and J. Kurchan, "Non-equilibrium glass transitions in driven and active matter", *Nat. Phys.*, 2013, **9**, 310–314.
- L. Berthier, "Nonequilibrium Glassy Dynamics of Self-Propelled Hard Disks", *Phys. Rev. Lett.*, 2014, **112**, 220602.
- R. Ni, M. A. Cohen Stuart and M. Dijkstra, "Pushing the glass transition towards random close packing using self-propelled hard spheres", *Nat. Commun.*, 2013, **4**, 2704.
- G. Szamel, E. Flenner and L. Berthier, "Glassy dynamics of athermal self-propelled particles: Computer simulations and a nonequilibrium microscopic theory", *Phys. Rev. E: Stat., Nonlinear, Soft Matter Phys.*, 2015, **91**, 062304.
- R. Mandal, P. J. Bhuyan, M. Rao and C. Dasgupta, "Active fluidization in dense glassy systems", *Soft Matter*, 2016, **12**, 6268–6276.
- L. Berthier, E. Flenner and G. Szamel, "Perspective: Glassy dynamics in dense systems of active particles", *J. Chem. Phys.*, 2019, **150**, 200901.
- N. Klongvessa, F. Ginot, C. Ybert, C. Cottin-Bizonne and M. Leocmach, "Active Glass: Ergodicity Breaking Dramatically Affects Response to Self-Propulsion", *Phys. Rev. Lett.*, 2019, **123**, 248004.
- L. Janssen, "Active glasses", *J. Phys.: Condens. Matter*, 2019, **31**, 503002.
- E. Flenner, G. Szamel and L. Berthier, "The nonequilibrium glassy dynamics of self-propelled particles", *Soft Matter*, 2016, **12**, 7136–7149.
- L. Berthier, E. Flenner and G. Szamel, "How active forces influence nonequilibrium glass transitions", *New J. Phys.*, 2017, **19**, 125006.
- Y.-E. Keta, J. U. Klamsner, R. L. Jack and L. Berthier, "Emerging mesoscale flows and chaotic advection in dense active matter", *Phys. Rev. Lett.*, 2024, **132**, 218301.
- Q. Liao and N. Xu, "Criticality of the zero-temperature jamming transition probed by self-propelled particles", *Soft Matter*, 2018, **14**, 853–860.
- J. D. Weeks, D. Chandler and H. C. Andersen, "Role of Repulsive Forces in Determining the Equilibrium Structure of Simple Liquids", *J. Chem. Phys.*, 1971, **54**, 5237–5247.
- G. Szamel, "Self-propelled particle in an external potential: Existence of an effective temperature", *Phys. Rev. E: Stat., Nonlinear, Soft Matter Phys.*, 2014, **90**, 012111.
- U. M. B. Marconi, N. Gnan, M. Paoluzzi, C. Maggi and R. Di Leonardo, "Velocity distribution in active particles systems", *Sci. Rep.*, 2016, **6**, 23297.
- E. Fodor, C. Nardini, M. E. Cates, J. Tailleur, P. Visco and F. van Wijland, "How Far from Equilibrium Is Active Matter?", *Phys. Rev. Lett.*, 2016, **117**, 038103.
- M. Paoluzzi, D. Levis and I. Pagonabarraga, "From motility-induced phase-separation to glassiness in dense active matter", *Commun. Phys.*, 2022, **5**, 111.
- A. W. Lees and S. F. Edwards, "The computer study of transport processes under extreme conditions", *J. Phys. C: Solid State Phys.*, 1972, **5**, 1921–1929.
- A. Gülce Bayram, L. Biancofiore, F. J. Schwarzendahl, H. Löwen and L. Biancofiore, "Motility-induced shear thickening in dense colloidal suspensions", *Soft Matter*, 2023, **19**, 4571–4578.
- G. Szamel, "Theory for the dynamics of dense systems of athermal self-propelled particles", *Phys. Rev. E*, 2016, **93**, 012603.
- A. Liluashvili, J. Ónody and T. Voigtman, "Mode-coupling theory for active Brownian particles", *Phys. Rev. E*, 2017, **96**, 062608.
- M. Feng and Z. Hou, "Mode coupling theory for nonequilibrium glassy dynamics of thermal self-propelled particles", *Soft Matter*, 2017, **13**, 4464–4481.



- 30 J. Reichert, L. F. Granz and T. Voigtmann, "Transport coefficients in dense active Brownian particle systems: mode-coupling theory and simulation results", *Eur. Phys. J. E: Soft Matter Biol. Phys.*, 2021, **44**, 27.
- 31 M. Feng and Z. Hou, "Mode-coupling theory for the dynamics of dense underdamped active Brownian particle system", *J. Chem. Phys.*, 2023, **158**, 024102.
- 32 V. E. Debets and L. M. C. Janssen, "Mode-coupling theory for mixtures of athermal self-propelled particles", *J. Chem. Phys.*, 2023, **159**, 014502.
- 33 A. K. Omar, K. Klymko, T. GrandPre and P. L. Geissler, "Phase Diagram of Active Brownian Spheres: Crystallization and the Metastability of Motility-Induced Phase Separation", *Phys. Rev. Lett.*, 2021, **126**, 188002.

